Block Ionomer Complexes of PEG-*block*-poly(4-vinylbenzylphosphonate) and Cationic Surfactants as Highly Stable, pH Responsive Drug Delivery System

Masao Kamimura [a,b], Jong Oh Kim [c], Alexander V. Kabanov [b,d,*], Tatiana K. Bronich [b,d*], and Yukio Nagasaki [a,e,f,*]

(a) Department of Materials Sciences, Graduate School of Pure and Applied Sciences, University of Tsukuba, Ten-noudai 1-1-1, Tsukuba, Ibaraki 305-8573, Japan
(b) Department of Pharmaceutical Sciences and Center for Drug Delivery and Nanomedicine, College of Pharmacy, University of Nebraska Medical Center, Omaha, NE 68198-5830, USA
(c) College of Pharmacy, Yeungnam University, 214-1 Dae-Dong, Gyeongsan 712-749, South Korea
(d) Laboratory of Chemical Design of Bionanomaterials, Department of Chemistry, M.V. Lomonosov Moscow State University, 119899 Moscow, Russia
(e) Master's School of Medical Sciences, Graduate School of Comprehensive Human Science, University of Tsukuba, Ten-noudai 1-1-1, Tsukuba, Ibaraki 305-8573, Japan
(f) International Center for Materials Nanoarchitectonics Satellite (WPI-MANA), National Institute for Materials Science (NIMS), University of Tsukuba, Ten-noudai 1-1-1, Tsukuba, Ibaraki 305-8573, Japan

*Corresponding authors:
A. V. Kabanov (Tel: +1-402-559-9364, Fax: +1-402-559-9365, e-mail: akabanov@unmc.edu)
T. K. Bronich (Tel: +1-402-559-9351, Fax: +1-402-559-9365, e-mail: tbronich@unmc.edu)
Y. Nagasaki (Tel: +81-29-853-5749, Fax: +81-29-853-5749, e-mail: yukio@nagalabo.jp)

KEYWORDS (6 words)
PEG
Surfactant-assisted Polymeric Micelle
Doxorubicin
Polyion complex
Micelle
Drug delivery

ABSTRACT

A new family of block ionomer complexes (BIC) formed by poly(ethylene glycol)-*block*-poly(4-vinylbenzylphosphonate) (PEG-*b*-PVBP) and various cationic surfactants was prepared and characterized. These complexes spontaneously self-assembled in aqueous solutions into particles with average size of 40 - 60 nm and remained soluble over the entire range of the compositions

of the mixtures including stoichiometric electroneutral complexes. Solution behavior and physicochemical properties of such BIC were very sensitive to the structure of cationic surfactants. Furthermore, such complexation was used for incorporation of cationic anti-cancer drug, doxorubicin (DOX), into the core of BIC with high loading capacity and efficiency. The DOX/PEG-*b*-PVBP BIC also displayed high stability against dilution, changes in ionic strength. Furthermore, DOX release at the extracellular pH of DOX/PEG-*b*-PVBP BIC was slow. It was greatly increased at the acidic pH mimicking the endosomal/lysosomal environment. Confocal fluorescence microscopy using live MCF-7 breast cancer cells suggested that DOX/PEG-*b*-PVBP BICs are transported to lysosomes. Subsequently, the drugs are released and exert cytotoxic effect killing these cancer cells. These findings indicate that the obtained complexes can be attractive candidates for delivery of cationic drugs to tumors.

INTRODUCTION

A very special class of drug delivery systems based on block and graft copolymers containing ionic and non-ionic water-soluble segments ("block ionomers") was proposed in mid-90-ies [1-4]. Such drug delivery systems are spontaneously formed in aqueous solutions upon electrostatic binding of block ionomer with oppositely charged molecules. The resulting complexes represent micelle-like particles termed "polyion complex micelles"[5-7], or "block ionomer complexes" (BICs) [8,9]. They have attracted great attention in various applications for delivery of low molecular mass drugs [10-13], proteins [14,15], polynucleotides (antisense oligonucleotides [16,17], plasmid DNA [18,19], siRNA [20,21]) and imaging agents [22,23]. For example, due to extended blood circulation and ability to circumvent renal excretion, known as the "enhanced permeability and retention (EPR) effect" [24,25], BICs loaded with anticancer drugs exhibit preferential accumulation and delivery of their cargos to solid tumors [26].

A special class of BICs was previously prepared by reacting block ionomers with surfactants of opposite charge, resulting in the spontaneous formation of the nanomaterials, which differ in sizes and morphologies, such as micelles and vesicles [27-34]. These materials contain a hydrophobic core formed by the surfactant tail groups and a hydrophilic shell formed by nonionic chains of the block copolymer (for example by PEG). These BICs can incorporate charged surfactant drugs, such as retinoic acid that binds to the polyelectrolyte chains, as well as hydrophobic non-charged drugs that solubilize in the hydrophobic domains formed by surfactant tail groups [35]. They display an ability to respond to the changes in the environmental parameters such as pH and ionic strength and can be designed to release drugs triggered by the environment in the target cell [36]. The simplicity of design and availability of diverse surfactant components for preparation of such BICs makes them quite attractive for development of carriers for drug delivery.

Here we explore BICs formed by anionic poly(ethylene glycol)-*block*-poly(4-vinylbenzylphosphonate) block ionomer (PEG-*b*-PVBP) and cationic surfactants (Scheme 1). The structure of PEG-*b*-PVBP is quite different compared to regular "double

hydrophilic" block ionomers, such as PEG-*block*-poly(methacrylic acid) (PEG-*b*-PMA), that were previously studied by us and others [37,38]. Specifically, the polyion segment of PEG-*b*-PVBP contains hydrophobic styrene moiety in every repeating unit, which can strongly affect the self-assembly and colloidal stability of the resulting BICs. Furthermore, in addition to a regular cationic surfactant we explored the use of a cationic surfactant drug, doxorubicin (DOX) for preparation of BICs. Since such BICs are potential drug delivery vehicles their loading efficacy with respect to DOX, the release rate of DOX at different environmental pH and *in vitro* cytotoxicity in cancer cells were also examined. Overall the results of this study further advance the potential use of BICs in drug delivery.

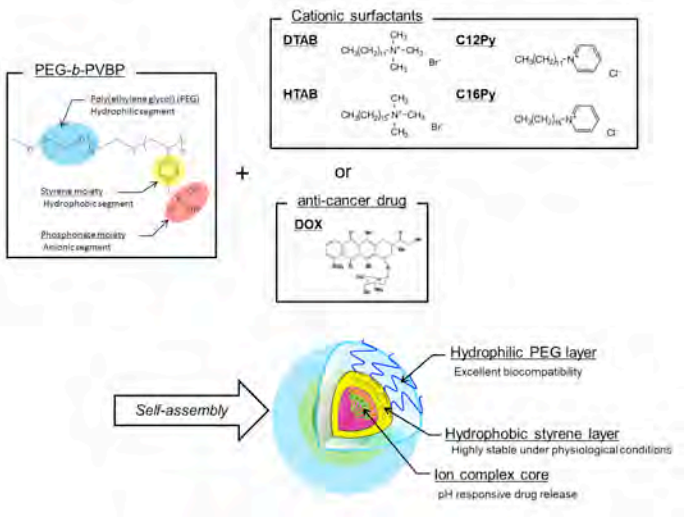

Scheme 1. Schematic illustration of self-assembly of the block ionomer complexes.

MATERIALS AND METHODS

Materials

PEG-*b*-PVBP block copolymer was synthesized as described in our previous report [39]. The repeating units for PEG and PVBP blocks were 113 and 20, respectively. Methanol, dodecyltrimethylammonium bromide (DTAB), hexadecyltrimethylammonium bromide (HTAB), and cetylpyridinium chloride (C16Py) were purchased from Sigma-Aldrich (St Louis, MO). Dodecylpyridinium chloride (C12Py) was purchased from Tokyo Chemical Industry, Co., Ltd, (Tokyo, Japan). Doxorubicin hydrochloride (DOX) was kindly provided by Dong-A Pharmaceutical Company (Korea). Lysotracker Green, fetal bovine serum (FBS), and Dulbecco's Modified Eagle's Medium (DMEM) were purchased from Invitrogen Inc (Carlsbad, CA). MTT reagent (3-(4,5-dimethylthiazol-2-yl)-2,5-diphenyltetrazolium bromide) was purchased from Research Products International (Mount Prospect, IL). All other chemicals were used without further purification.

Preparation of BICs formed by PEG-*b*-PVBP and cationic surfactants

Cationic surfactants (DTAB, HTAB, C12Py, and C16Py) and PEG-*b*-PVBP were separately dissolved in water and methanol, respectively. Their concentrations were 50 mM and 22 mM, respectively. An aqueous solution surfactant and water were added to a vial followed by addition of 0.2 mL of PEG-*b*-PVBP solution in methanol to achieve the desired composition of the mixture. Final volume of the solution was adjusted to 2.4 mL with water. Methanol was removed by evaporation. The composition of the mixture (Z value) was expressed as the molar ratio of the concentration of the surfactant to the concentration of 4-vinylbenzylphosphonate (VBP) units, Z = [surfactant]/[VBP]. For example, when the 0.088 mL of surfactant solution was mixed with 0.2 mL of PEG-*b*-PVBP solution, the Z value of the mixture was 1.0. Surfactant composition of the BIC is labeled in accordance with the surfactant nomenclature, i.e. DTAB/PEG-*b*-PVBP refers to the BIC formed from DTAB surfactant and copolymer.

Fluorescence measurements

Fluorescence spectra and intensity measurements were carried out using Fluorolog3 (Horiba Jobin Yvon, France). Pyrene solubilization method was used to detect the onset of surfactant aggregation [40,41]. The known amounts of pyrene in acetone were added to empty vials, followed by acetone evaporation. Solutions of surfactants or surfactant/PEG-*b*-PVBP mixture in phosphate buffer (10 mM, pH7.0) containing 5 vol% of methanol were added to the vials and kept overnight under constant stirring at room temperature. Pyrene concentration in the final solution was 0.95 μM. Pyrene fluorescence spectra were recorded at λ_{ex} = 336 nm, λ_{em} = 340 – 460 nm, and bandwidth of 2.5 nm for excitation and emission. All measurements were performed at room temperature.

Size and ζ-potential measurements

Effective mobility and z-averaged hydrodynamic diameters of the BICs were determined by dynamic light scattering (DLS) using ZetasizerNano ZS (Malvern Instruments, U.K.) equipped with a He-Ne laser that operated at a wavelength of 635 nm. Measurements were performed at a detection angle of 173º at room temperature. ζ-potential of the particles was calculated from the electrophoretic mobility value using Smoluchowski equation. Software provided by the manufacturer which employs cumulants analysis and non-negatively constrained least-squares particle size distribution analysis routines was used to analyze the size of the particles, polydispersity indices (PDI), and ζ-potential. The mean values were calculated from the measurements performed at least in triplicate.

Atomic Force Microscopy (AFM) measurements

AFM imaging was performed in air using a Multimode NanoScope IV system (Veeco, Santa Barbara, CA) operating in a tapping mode. The unbound surfactant and large aggregates were separated from the BICs solutions using NAP column (GE Healthcare, US) and 0.22 μm filter

purification before AFM measurement. The samples were prepared by depositing 5 μL of BICs solutions onto positively charged 1-(3-aminopropyl)silatrane mica surface (APS mica) for 2 min followed by drying the surface under argon atmosphere. The imaging was performed with regular etched silicon probes (TESP) with a spring constant of 42 N/m. The images were processed and the widths and heights of the particles were measured using FemtoScan software (Advanced Technologies Center, Moscow, Russia).

Preparation of DOX and PEG-*b*-PVBP complex

DOX/PEG-*b*-PVBP BICs were prepared using a procedure similar to the one described above for surfactant/PEG-*b*-PVBP. Briefly, 0.2 mL of PEG-*b*-PVBP solution in methanol was added to aqueous solution of DOX, and final volume of the mixture was adjusted to 2.4 mL with water. Methanol was removed by evaporation. The composition of the mixture was expressed as the molar ratio of the DOX concentration to the concentration of VBP units, Z = [DOX]/[VBP]. The unbound DOX was removed by ultrafiltration using Amicon Ultra-4 centrifugal filter devices (MWCO 10000 Da, Millipore) pretreated with DOX. The final concentration of DOX in the BIC dispersions was determined by measuring the absorbance at 485 nm using Lambda 25 UV/VIS spectrophotometer.

Release studies of DOX

Release of DOX from the DOX/PEG-*b*-PVBP BICs was examined in acetate buffer saline (ABS) (pH5.5, 145 mM NaCl), phosphate buffer saline (PBS) (pH7.4, 145 mM NaCl), and DMEM media (pH7.4, 145 mM NaCl, 10 % FBS) at 37 ºC by dialysis method using a membrane (MWCO 3,500 Da). At definite time intervals (1 – 48 h), 1 mL samples of the dialysate solution were withdrawn and replaced with an equal volume of fresh media. The concentration of DOX in dialysate samples was determined spectrophotometrically by measuring absorbance at 485 nm. The amount of DOX released from the BICs was expressed as a percentage of the total DOX and plotted as a function of time.

***In vitro* cytotoxicity studies**

Cytotoxicity of DOX/PEG-*b*-PVBP BIC was assessed human breast cancer cell line MCF-7 by a standard MTT assay. Briefly, cells were seeded in a 96-well microtiter plates with 5000 cells per well and allowed to adhere for 24 h prior to the assay. Cells were exposed to various doses (0 – 200 μg/mL on DOX basis) of DOX alone, PEG-*b*-PVBP micelles alone, and DOX/PEG-*b*-PVBP BIC for 24 h at 37 ºC, followed by washing with PBS, and maintaining in RPMI 1640 medium with 10 % FBS for additional 72 h. The 25μL of MTT indicator dye (5 mg/mL) was added to each well and the cells were incubated for 2 h at 37 ºC in the dark. The 100 μL of 50 % DMF-20% SDS solution was added to each well and kept overnight at 37 ºC. Absorption was measured at 570 nm in a microplate reader (SpectraMax M5, Molecular Devices

Co., US) using wells without cells as blanks. All measurements were taken eight times.

Confocal microscopy on live cell

Cellular uptake of DOX/PEG-*b*-PVBP BIC was characterized by live cell confocal imaging using Carl Zeiss LSM 510 Meta Confocal microscope (Peabody, MA). MCF-7 cells were plated in live cell chambers (Fischer Scientific, Waltham, MA) and after two days (37 ºC, 5 % CO_2) exposed to DOX/PEG-*b*-PVBP BIC for 30 min, followed by incubation with Lysotracker Green for 5 min. Finally, cells were washed and kept in complete media for confocal imaging.

RESULTS AND DISCUSSION

Formation of BIC as a function of surfactant concentrations

The interaction between PEG-*b*-PVBP and various cationic surfactants was characterized by steady-state fluorescence using pyrene as a probe. The ratio of intensities of the first and third highest energy emission peaks in the pyrene spectrum (I_1/I_3 ratio) correlates with the polarity of the immediate environment of the pyrene probe. In aqueous solution the I_1/I_3 ratio is about 1.7-1.9 while in a nonpolar solvent such as hexane it is about 0.6 [41]. In a typical surfactant solution below the critical micelle concentration (cmc) the I_1/I_3 value is the same as that in water. When the concentration of surfactant exceeds the cmc, the I_1/I_3 ratio drops significantly, indicating the incorporation of pyrene into the nonpolar interior of the micelle.

Table 1. Micellar Characteristics of Various Cationic Surfactants without[a] and in the Presence[b] of PEG-*b*-PVBP

	DTAB	HTAB	C12Py	C16Py
cmc (M)[a]	2.5×10^{-3}	1.1×10^{-4}	7.0×10^{-4}	5.0×10^{-4}
cac (M)[b]	1.5×10^{-4}	2.8×10^{-5}	6.0×10^{-5}	4.0×10^{-5}

Association behavior of PEG-*b*-PVBP copolymer was examined using fluorescence measurements. The I_1/I_3 fluorescence intensity ratio of pyrene in PEG-*b*-PVBP solution depended on the copolymer concentration (Supplementary Information, Figure S1). Due to the presence of methanol in the sample solutions (5 vol%), the environment of pyrene probe was less polar than in the pure water and was characterized by the I_1/I_3 ratio 1.53 even in the absence PEG-*b*-PVBP copolymer. As the concentration of PEG-*b*-PVBP increased this copolymer alone formed micelles with the cmc value of 4.4×10^{-5} M (0.4 mg/mL), which was determined by the onset of sharp decrease of I_1/I_3 ratio value.

The interaction between polyions and oppositely charged surfactants is a cooperative process in which the surfactant ionic head groups bind to the polyion units while the surfactant alkyl tails segregate into a hydrophobic microphase. This process is characterized by “critical association concentration” (cac), corresponding to the onset of surfactant binding to the polymer. As seen in

Figure S2 in Supplementary Information for various surfactant/PEG-*b*-PVBP mixtures the I_1/I_3 ratio remained practically constant or only slightly changed below the cac. Above the cac the I_1/I_3 decreased significantly reflecting the partitioning of the pyrene into the hydrophobic environment formed by the surfactant alkyl groups. The dependencies of the I_1/I_3 ratio vs. concentration for each surfactant in the polymer-free systems are also presented in Figure S2 in Supplementary Information for comparison. For all surfactants studied the cac values determined in the presence of PEG-*b*-PVBP copolymer were about one order of magnitude lower than the corresponding cmc (Table 1). This suggested that PEG-*b*-PVBP enhanced the surfactant aggregation as a result of electrostatic coupling of the surfactant head groups and polyion repeating units.

Characterization of BICs

The surfactant/PEG-*b*-PVBP BICs were characterized on a macroscopic level by photon correlation spectroscopy and laser microelectrophoresis technique at various compositions of the mixture. Figure 1 presents averaged particle size, polydispersity, and ζ-potential of BICs as a function of Z at various pH values. Notably, no precipitation in BIC dispersions was observed over the entire range of the studied compositions of the mixture. In all cases, hydrodynamic diameters and polydispersity of BIC particles were about 50 nm and 0.3, respectively. These values remained practically constant upon variations of the composition of the mixture ($0.5 \leq Z \leq 2.0$) and pH from 5.0 to 8.0. Steric repulsion of the PEG chains prevents the BICs from secondary agglomeration, retaining the high solubility of the BICs in aqueous solutions

It is also important to note that there were little if any differences in ζ-values for all BICs at different pH, from pH5.0 to pH8.0 (Figure 1 (c)). In all cases, ζ-values were negative at $Z < 1$. Therefore, only a part of PVBP chain was neutralized by the surfactant under these conditions, while the remaining ionized phosphonate groups provided for the net negative charge of the particles. As Z value increased the value of ζ-potential is also increased due to progressive neutralization of PVBP units by surfactant cations. Notably, in the case of cationic surfactants having relatively long alkyl chains (HTAB and C16Py), ζ-potential reached 0 in the vicinity of $Z = 1$ suggesting that practically all surfactant ions present in the system formed salt bonds with phosphonate groups of PEG-*b*-PVBP. At $Z > 1$, the particles of BIC formed in HTAB/PEG-*b*-PVBP and C16Py/PEG-*b*-PVBP mixtures became positively charged. The change in the sign of the ζ-potential indicated the incorporation of an excess of surfactant into the BIC particles. Indeed, the fraction of unbound C16Py in the solution was practically constant in the entire range of the compositions of mixture studied (Supplementary Information, Figure S3). It is likely that the aliphatic tails of the surfactant inserted into the hydrophobic domains of the BIC while the ionic head groups were exposed to water. Similar behavior was previously described for regular BIC of various block copolymers and oppositely charged surfactants [9,42]. However, the less hydrophobic surfactants with shorter aliphatic groups (DTAB and C12Py) exhibited reduced ability for incorporation into the BICs at the surfactant excess. In these cases the net charge of the

particles leveled-off close to zero only in the vicinity of Z = 2.0. No inversion of the charge was observed for DTAB/PEG-*b*-PVBP and C12Py/PEG-*b*-PVBP mixtures at the excess of added surfactant. Furthermore, the fraction of unbound surfactant (C12Py) increased as Z value increased (Supplementary Information, Figure S3) suggesting that the excess of surfactant did not incorporate into the complex and coexisted with the BICs in dispersion.

We performed the further characterization of surfactant/PEG-*b*-PVBP BICs by using electrostatically neutralized BICs. At Z value was around 1.0, ζ-potential values of various surfactant/PEG-*b*-PVBP BICs were reached to around 0 mV (Figure 1 (c)). Thus, we have focused on the Z = 1.0 for further characterization of surfactant/PEG-*b*-PVBP BICs. The size and shape of the BICs were further characterized by the tapping-mode AFM. The typical images of BICs formed by PEG-*b*-PVBP and cationic surfactants (HTAB and C16Py) showed round nanoparticles (Figure 2). The number-average particle diameters of 30.20 ± 3.56 nm and 33.35 ± 5.08 nm were determined for HTAB/PEG-*b*-PVBP and C16Py/PEG-*b*-PVBP BICs deposited on mica, respectively. It is reported that micelle size and its distribution tend to decrease during drying process [38]. Thus, smaller size and size distribution of BICs in AFM analysis are probably due to drying process on mica.

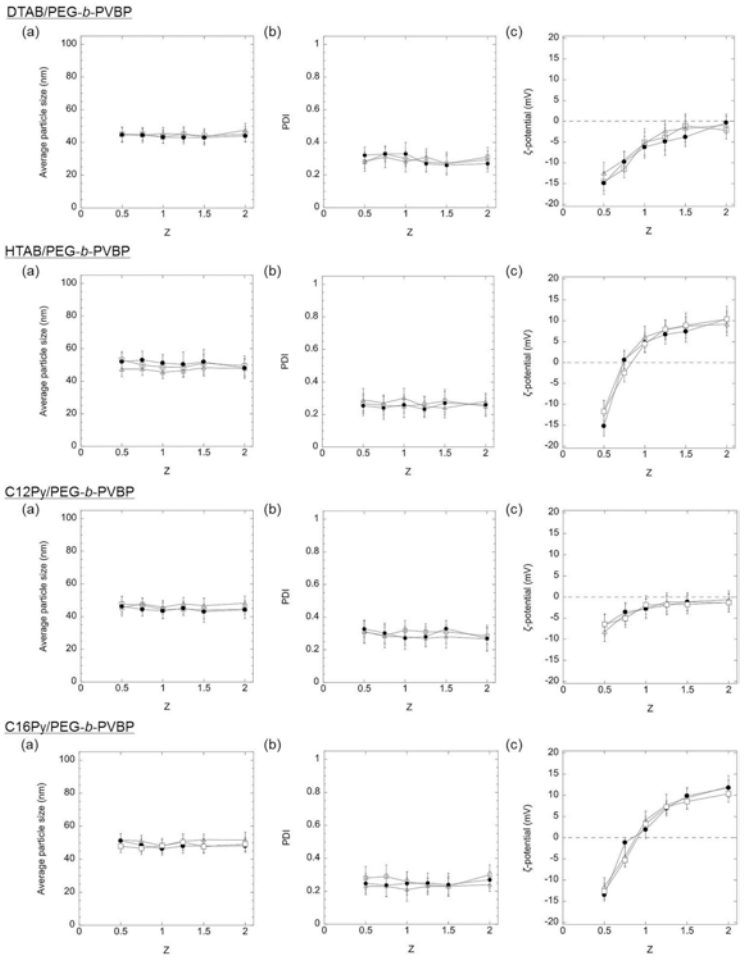

Figure 1. Average hydrodynamic diameter (a), PDI (b), and ζ-potential (c) of BICs at various pH

and compositions of the mixture, Z: pH5.0 (open triangles), pH7.0 (filled circles), and pH8.0 (open squares). The data presented as mean ± SD (n = 5).

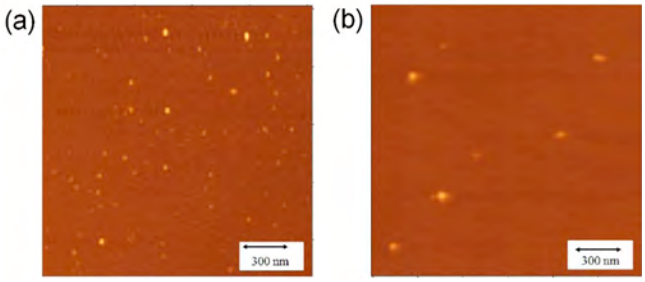

Figure 2. Tapping mode AFM images in air of (a) HTAB/PEG-*b*-PVBP BIC and (b) C16Py/PEG-*b*-PVBP BIC. Composition of the surfactant/PEG-*b*-PVBP was Z = 1.0, pH7.0.

Effect of salt concentration on BICs

Addition of low molecular weight of salts to complexes of electrolytes with oppositely charged surfactants usually leads to destabilization of the salt bonds. Figure 3 presents the DLS graphs of the particles size distribution of various BICs (Z = 1.0) at different concentrations of the added NaCl. PEG-*b*-PVBP micelles alone displayed formation of large aggregates at the physiological concentration of the salt, which was further enhanced as the salt concentrations increase. In this case it was possible that the sodium counter ions screened the phosphonate groups of PVBP chains and decreased their electrostatic repulsion, thus favoring increased aggregation of PEG-*b*-PVBP at the higher ionic strength. On the other hand, addition of salt could have decreased the quality of water as a solvent for PEG, thus, decreased PEG steric stabilizing capacity, also favoring formation of large aggregates. Similarly, formation of larger aggregates and increases in particle polydispersity observed in DTAB/PEG-*b*-PVBP BICs, albeit at much higher concentrations of added salt (around 0.66 M). Such behavior was not seen for the C12Py/PEG-*b*-PVBP BICs, which displayed practically same sizes and polydispersity values in the entire range of salt concentrations studied. At the same time, the amount of the unbound C12Py surfactant was increased nearly 2-fold in 0.15 M solution of NaCl compared to C16Py surfactant (Supplementary Information, Figure S4). Upon further increase in salt concentration up to 1 M there was no additional release of surfactant ions from the BICs. Based on the observed differences in behavior of DTAB/PEG-*b*-PVBP BICs and C12Py/PEG-*b*-PVBP BICs in response to added salt it seems reasonable to attribute a higher stability of BIC formed by C12Py surfactants to the additional hydrophobic interactions of the pyridinium moieties with benzyl groups in VBP units. In the case of BIC formed by surfactants with longer alkyl chains, no differences in particle size/polydispersity were observed for either HTAB/PEG-*b*-PVBP or C16Py/PEG-*b*-PVBP BICs (Figure 3). In addition, the fraction of unbound C16Py in the solution did not change in the entire range of the salt concentration (Supplementary Information, Figure S4). Altogether, the effects of added salt suggested that the stability of BICs formed in the surfactant/PEG-*b*-PVBP mixtures depended on

the structure of ionic head group and alkyl tails of the surfactant. The surfactants with either 1) longer alkyl tail or 2) aromatic head group formed the more stable complex.

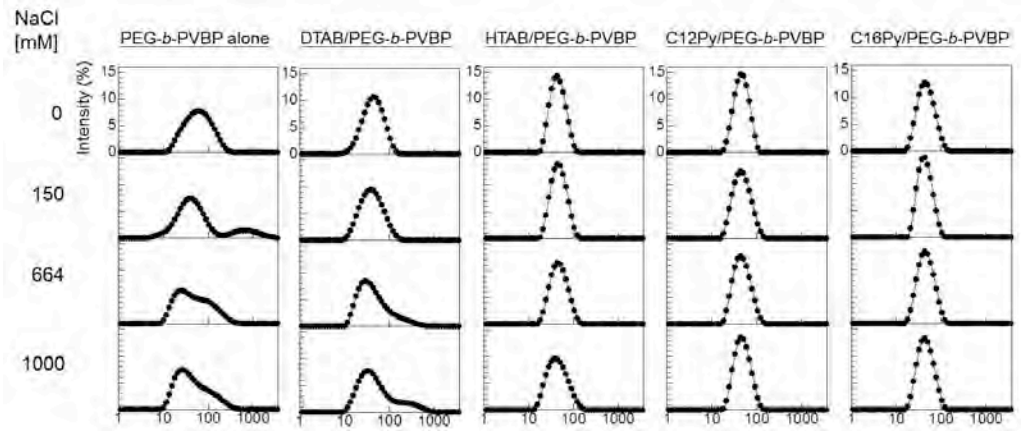

Figure 3. Dependence of particle size distribution of BICs on the concentration of NaCl. Composition of the surfactant/PEG-*b*-PVBP mixture was Z = 1.0, the concentration of PEG-*b*-PVBP was 1.83 mmol/L, pH7.0, r.t..

Preparation of DOX and PEG-*b*-PVBP complex

We evaluated a possibility to immobilize a cationic anti-cancer drug (DOX, pKa = 8.2) into BICs based on PEG-*b*-PVBP. The complexes were prepared by mixing the aqueous solution of DOX and methanol solution of block copolymer at pH7.0. The average hydrodynamic diameter and ζ-potential of the complexes obtained at various compositions of the mixtures are presented in Figure 4. Similarly to the surfactant/PEG-*b*-PVBP BIC, the average hydrodynamic diameters and polydispersity of DOX/PEG-*b*-PVBP BIC remained practically constant (ca. 50 nm and 0.25, respectively) upon variations of the composition of the mixture ($0.1 \leq Z \leq 1.0$) (Figure 4(a)). At $Z < 1$ ζ-potential of the BICs was increases as the concentration of the added DOX (Figure 4(b)). Nearly all added DOX molecules were incorporated into BIC since practically no unbound DOX was detected in the solution at $0.1 \leq Z \leq 1.0$ (Supplementary Information, Figure S5).

We performed the further characterization of DOX/PEG-*b*-PVBP BICs by using electrostatically neutralized BICs. At $Z \geq 0.5$, ζ-potential value of DOX/PEG-*b*-PVBP BICs was around 0 mV (Figure 4 (b)). Thus, we have focused on the Z = 0.5 for further characterization of DOX/PEG-*b*-PVBP BICs. The binding of DOX with PEG-*b*-PVBP was also supported by quenching of DOX fluorescence (by ca. 80 %) compared to the fluorescence of free DOX in an aqueous solution (Figure 4(c)). Substantial reduction in DOX fluorescence intensity can be attributed to the self-association of DOX molecules bound to the PVBP chains within the core of complexes. Overall, total drug loading of about 35.7 % wt. was obtained (expressed as mass of incorporated DOX per mass of DOX/PEG-*b*-PVBP mixtures). AFM suggested that BICs particles formed in these mixtures appeared to be spherical with a number-averaged height of 2.17 ± 0.41 nm and diameter of 42.31 ± 2.38 nm (Figure 4(d)).

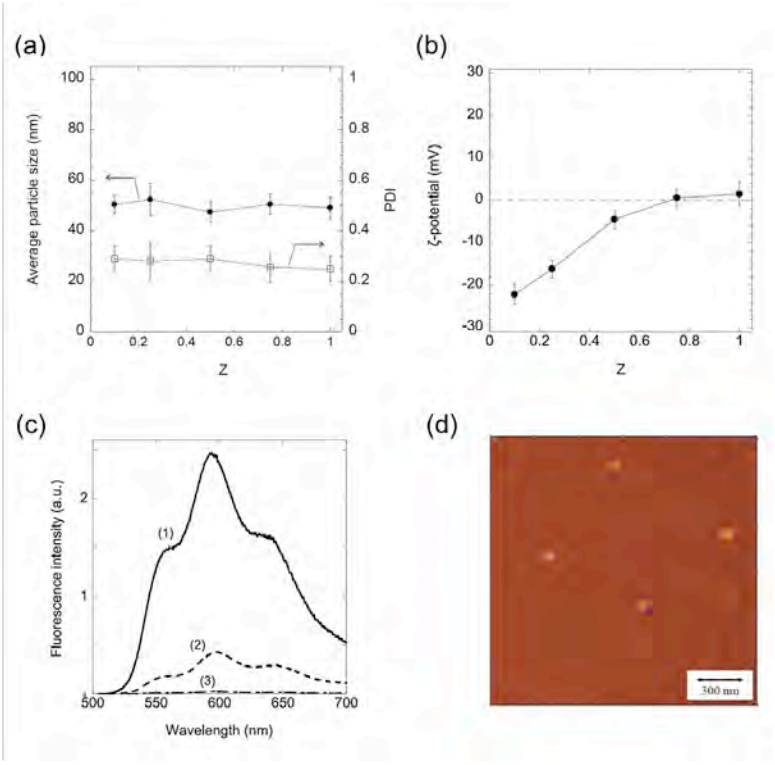

Figure 4. Average hydrodynamic diameter (filled circles) and PDI (open squares) (a) and ζ-potential (b) of DOX/PEG-*b*-PVBP BIC. The data presented as mean ± SD (n = 5). (c) Fluorescence emission spectra of free DOX (1), DOX/PEG-*b*-PVBP BIC (2), and PEG-*b*-PVBP alone (3). (d) Tapping mode AFM image in air of DOX/PEG-*b*-PVBP BIC. Composition of the DOX/PEG-*b*-PVBP mixture was Z = 0.5, pH7.0, r.t..

Salt and serum stability of DOX/PEG-*b*-PVBP BICs

Figure 5(a) presents the dependence of particle size and polydispersity of DOX/PEG-*b*-PVBP BIC (Z = 0.5) on the concentration of NaCl. The averaged diameter and polydispersity of these BICs did not change in the entire range of the salt concentrations studied (up to 1 M). In addition, DOX/PEG-*b*-PVBP BICs showed very little if any release of DOX: less than 2 % of unbound DOX was detected in the BIC dispersions at high salt concentrations (Supplementary Information, Figure S6). These data suggested that DOX/PEG-*b*-PVBP BICs were remarkably stable. In comparison, BICs formed in DOX/PEG-*b*-poly(methacrylic acid) mixture displayed progressive disintegration in the presence of salt followed by their complete disappearance at 0.13 M NaCl.[35] Furthermore, DOX/PEG-*b*-PVBP BICs were stable in the presence of 10 % FBS in the buffer (Figure 5(b)) and no changes in particle size and polydispersity of these BICs were determined for at least a week. As in the case of surfactant/PEG-*b*-PVBP BICs, such high stability of DOX/PEG-*b*-PVBP BIC in both salt and serum solution was probably due to

that the core of DOX/PEG-*b*-PVBP BIC was stabilized by both electrostatic and hydrophobic interactions.

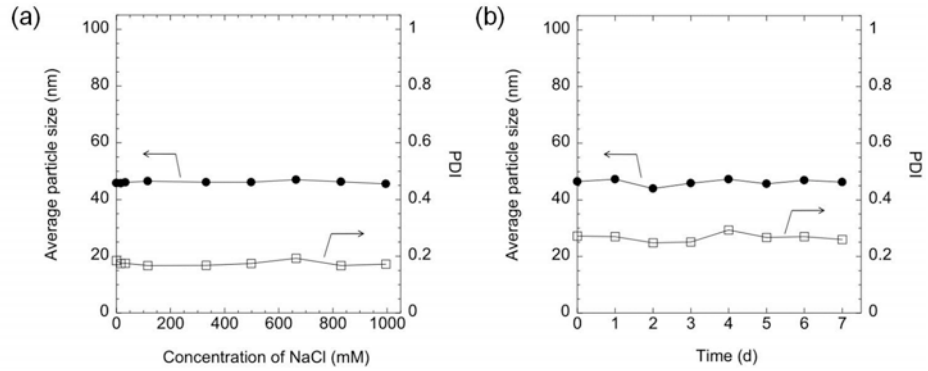

Figure 5. (a) Dependence of average particle size (filled circles) and PDI (open squares) of DOX/PEG-*b*-PVBP BIC on the concentration of NaCl. (b) Time dependence of the average particle size (filled circles) and PDI (open squares) of DOX/PEG-*b*-PVBP BIC in 10 % FBS solution (10 mM phosphate buffer, pH7.4, 150 mM NaCl, 10 % FBS). Composition of the DOX/PEG-*b*-PVBP was Z = 0.5, pH7.0, r.t..

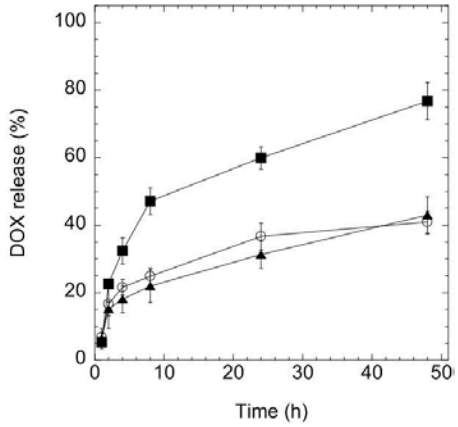

Figure 6. Time- and pH-dependent DOX release profiles of the DOX/PEG-*b*-PVBP BIC in (filled squares) ABS (pH5.5), (open circles) PBS (pH7.4), and (filled triangles) DMEM (pH7.4, 10 % FBS). The data presented are mean ± SD (n = 3). Composition of the DOX/PEG-*b*-PVBP mixture was Z = 0.5.

Release of DOX from BIC

The DOX release from the DOX/PEG-*b*-PVBP BIC was pH-dependent with the rate of the release being much faster at acidic pH5.5 than at neutral pH7.4 (Figure 6). At pH7.4 there was a small initial burst release of DOX (ca. 15 %) from DOX/PEG-*b*-PVBP BIC followed by slow and practically linear release of nearly 40 % of the drug over 50 h. Furthermore the release profile at neutral pH did not seem to be affected by the presence of the serum. In contrast at pH5.5 nearly 45 % of DOX was released during first 8 h. Such release profile at lower pH is noteworthy considering that the pH

in the endosomes and lysosomes are in the range of pH5 to pH6. The pK_a value of PEG-*b*-PVBP is both pK_{a1} = 2.1 and pK_{a2} = 7.2, respectively. At the neutral conditions, about 25 % of phosphonate groups were protonated. On the other hand, at the acidic pH conditions (pH5-6), about 45 – 55 % of phosphonate groups were protonated. Therefore, the accelerated DOX release from DOX/PEG-*b*-PVBP BIC at the acidic pH was probably due to the protonation of phosphonate groups of PVBP chains in the DOX/PEG-*b*-PVBP BICs.

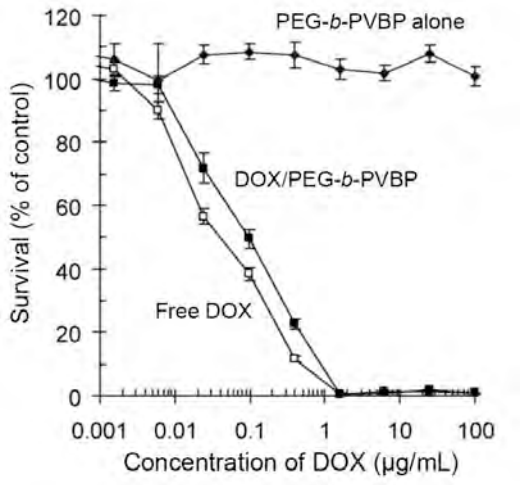

Figure 7. *In vitro* cytotoxicity of DOX/PEG-*b*-PVBP BIC against MCF-7 cells. (Filled circles) PEG-*b*-PVBP alone, (filled squares) DOX/PEG-*b*-PVBP BIC, and (open squares) free DOX. Composition of the DOX/PEG-*b*-PVBP mixture was Z = 0.5, pH7.0. The data presented as mean ± SD.

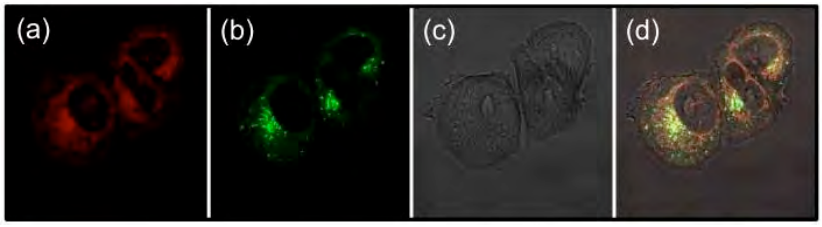

Figure 8. Fluorescence microscope images of the MCF-7 cells incubated with DOX/PEG-*b*-PVBP BIC. (a) DOX, (b) Late endosome or lysosome, (c) DIC, and (d) merged image. Composition of the DOX/PEG-*b*-PVBP mixture was Z = 0.5, pH7.0.

In Vitro Cytotoxicity and Intracellular Delivery

Cytotoxic activity of DOX/PEG-*b*-PVBP BIC was assessed against human MCF-7 breast cancer cells (Figure 7). The cell viability was progressively reduced as the concentration of free DOX or DOX/PEG-*b*-PVBP BIC increased. However, DOX incorporated into the complexes displayed lower cytotoxic effect on the cancer cells than the free DOX. Importantly, it was found that PEG-*b*-PVBP alone was not toxic in the entire range of concentrations used for the treatment

with DOX/PEG-*b*-PVBP complex formulation.

Furthermore, cellular uptake of the DOX/PEG-*b*-PVBP BIC was characterized by live cell confocal imaging. In the case of free DOX, an increase in nuclear fluorescence intensity in the MCF-7 cells was observed for 30 min incubation as shown in Figure S7 in Supplementary Information, indicating the binding of DOX to the nuclear DNA. The DOX/PEG-*b*-PVBP BIC was also readily internalized into MCF-7 cells after 30 min incubation (Figure 8). However, significant co-localization of DOX/PEG-*b*-PVBP BIC with Lysotracker Green, a marker of late endosome and lysosome, was observed (Figure 8(d)) in this case. This result indicated that DOX/PEG-*b*-PVBP BIC was probably taken up by MCF-7 cells via the endocytic pathway and retained in the late endosome or lysosome. In acidic compartment such as lysosome, the release of DOX was accelerated with time due to the protonation of phosphonate groups of PVBP chains.

CONCLUSIONS

BICs formed by PEG-*b*-PVBP and several cationic surfactants were successfully prepared. These complexes spontaneously self-assemble in aqueous solutions into particles with average size of 40 - 60 nm. The size and ζ-potential of these complexes were not affected by variation in pH. The cac value was about 1 order of magnitude lower than the cmc. Furthermore, the stability of such complexes was not affected by added salt up to 1 M concentration. Because of PEG-*b*-PVBP possess hydrophobic styrene moieties, the formed complexes were stabilized by not only electrostatic but also by hydrophobic interactions. Moreover, PEG-*b*-PVBP was used for immobilization and drug delivery of DOX. The DOX/PEG-*b*-PVBP BIC also displayed high stability against dilution, changes in ionic strength. The DOX/PEG-*b*-PVBP BIC showed almost no initial burst release of the DOX under physiological extracellular pH, albeit whereas significant release of DOX from DOX/PEG-*b*-PVBP BIC was observed at the acidic pH mimicking the endosomal/lysosomal environment. The cytotoxic activity of the DOX/PEG-*b*-PVBP BIC against the MCF-7 cancer cells was lower than that of the free DOX, which was consistent with the sustained release of DOX from the complexes. DOX/PEG-*b*-PVBP BIC was readily internalized into MCF-7 cells after 30 min incubation. Furthermore, co-localization of DOX/PEG-*b*-PVBP BIC with Lysotracker was observed in MCF-7 cells, which indicated that DOX/PEG-*b*-PVBP BIC reached late endosome or lysosome. From these findings, the obtained complexes are promising as novel nanocarriers for drug delivery.

ACKNOWLEDGMENT

We are grateful to Dr. Luda Shlyakhtenko for assistance with AFM studies; Mrs. Daria Filonova Alakhova and Mrs. Yi Zhao for assistance with confocal studies. This work was supported by NIH COBRE Nebraska Center for Nanomedicine (Grant 1P20RR021937). M.K. is also grateful for the research fellowships of the Japan Society for the Promotion of Science (JSPS) for Young Scientists.

REFERENCES

[1] E. V. Batrakova, T. K. Bronich, J. A. Vetro, A. V. Kabanov, Polymer micelles as drug carriers, *Nanoparticulates as Drug Carriers*, Imperial College Press, London, 2006, pp. 57-93.

[2] K. Kataoka, A. Harada, Y. Nagasaki, Block copolymer micelles for drug delivery: design, characterization and biological significance, *Adv. Drug Delivery Rev.* 47 (2001) 113–131.

[3] A. Lavasanifar, J. Samuel, G. S. Kwon, Poly(ethylene oxide)-block-poly(L -amino acid) micelles for drug delivery, *Adv. Drug Delivery Rev.* 54 (2002) 169–190.

[4] G. Riess, Micellization of block copolymers, *Prog. Polym. Sci.* 28 (2003) 1107–1170.

[5] A. Harada, K. Kataoka, Formation of Polyion Complex Micelles in an Aqueous Milieu from a Pair of Oppositely-Charged Block Copolymers with Poly(ethy1ene glycol) Segments, *Macromolecules* 28 (1996) 5294-5299.

[6] A. Harada. K. Kataoka, Chain Length Recognition: Core-Shell Supramolecular Assembly from Oppositely Charged Block Copolymers, *Science* 283 (1999) 65-67.

[7] A. Harada, K. Kataoka, Supramolecular assemblies of block copolymers in aqueousmedia as nanocontainers relevant to biological applications, *Prog. Polym. Sci.* 31 (2006) 949-982.

[8] A. V. Kabanov, T. K. Bronich, V. A. Kabanov, K. Yu, A. Eisenberg, Soluble Stoichiometric Complexes from Poly(*N*-ethyl-4-vinylpyridinium) Cations and Poly(ethylene oxide)-*block*-polymethacrylate Anions, *Macromolecules* 29 (1996) 6797-6802.

[9] T. K. Bronich, A. V. Kabanov, V. A. Kabanov, K. Yu, A. Eisenberg, Soluble Complexes from Poly(ethylene oxide)-*block*-polymethacrylate Anions and *N*-Alkylpyridinium Cations, *Macromolecules* 30 (1997) 3519-3525.

[10] M. L. Adams, A. Lavasanifar, G. S. Kwon, Amphiphilic Block Copolymers for Drug Delivery, *J. Pharm. Sci.* 92 (2003) 1343-1355.

[11] N. Rapoport, Physical stimuli-responsive polymeric micelles for anti-cancer drug delivery, *Prog. Polym. Sci.* 32 (2007) 962–990.

[12] Y. Bae, K. Kataoka, Intelligent polymeric micelles from functional poly(ethylene glycol)-poly(amino acid) block copolymers, *Adv. Drug Delivery Rev.* 61 (2009) 768-784.

[13] J. H. Park, G. Saravanakumar, K. Kim, I. C. Kwon, Targeted delivery of low molecular drugs using chitosan and its derivatives, *Adv. Drug Delivery Rev.* 62 (2010) 28-41.

[14] E. V. Batrakova, S. Li, A. D. Reynolds, R. L. Mosley, T. K. Bronich, A.V. Kabanov, H. E. Gendelman, A Macrophage-Nanozyme Delivery System for Parkinson's disease, *Bioconjugate Chem.* 18 (2007) 1498-1506.

[15] Y. Lee, S. Fukushima, Y. Bae, S. Hiki, T. Ishii, K. Kataoka, A protein Nanocarrier from Charge-Conversion Polymer in Response to Endosomal pH, *J. Am. Chem. Soc*. 129 (2007) 5362-5363.

[16] A. V. Kabanov, S. V. Vinogradov, Y. G. Suzdaltseva, V. Y. Alakhov, Water-soluble block polycations for oligonucleotide delivery, *Bioconjugate Chem.* 6 (1995) 639-643.

[17] Y. Kakizawa, K. Kataoka, Block copolymer micelles for delivery of gene and related

compounds, *Adv. Drug Delivery Rev.* 54 (2002) 203–222.
[18] H-K. Nguyen, P. Lemieux, S. Vinogradov, C. L. Gebhart, N. Guérin, G. Paradis, T. K. Bronich, V. Y. Kabanov, A. V. Kabanov, evaluation of polyether-polyethyleneimine graft copolymers as gene transfer agents, *Gene Ther.* 7 (2000), 126-138.
[19] N. Nishiyama, K. Kataoka, Current state, achievements, and future prospects of polymeric micelles as nanocarriers for drug and gene delivery, *Pharm. Therap.* 112 (2006) 630-648.
[20] W. J. Kim, S. W. Kim, Efficient siRNA Delivery with Non-viral Polymeric Vehicles, *Pharm. Res*. 26 (2009) 657-666.
[21] A. Tamura, Y. Nagasaki, Smart siRNA delivery systems based on polymeric nanoassemblies and nanoparticles, *Nanomedicine* 5 (2010) 1089-1102.
[22] M. Ji, L. Jin, J. Guo, W. Yang, C. Wang, S. Fu, Formation of luminescent nanocomposite assemblies via electrostatic interaction, *J. Colloid Interface Sci.* 318 (2008) 487–495.
[23] K. Shiraishi, K. Kawano, Y. Maitani, M. Yokoyama, Polyion complex micelle MRI contrast agents from poly(ethylene glycol)-b-poly(L-lysine) block copolymers having Gd-DOTA; preparations and their control of T1-relaxivities and blood circulation characteristics, *J. Controlled Release* 148 (2010) 160–167.
[24] Y. Matsumura, H. Maeda, A new Concept for Macromolecular Therapeutics in Cancer Chemotherapy : Mechanism of Tumoritropic Accumulation of Proteins and the Antitumor Agent Smancs, *Cancer Res.* 46 (1986) 6387-6392.
[25] H. Maeda, J. Wu, T. Sawa, Y. Matsumura, K. Hori, Tumor vascular permeability and the EPR effect in macromolecular therapeutics: a review, *J. Controlled Release* 65 (2000) 271–284.
[26] H. Maeda, Tumor-Selective Delivery of Macromolecular Drugs via the EPR Effect:Background and Future Prospects, *Bioconjugate Chem.* 21 (2010) 797–802.
[27] S. Zhou, H. Hu, C. Burger, B. Chu, Phase Structural Transitions of Polyelectrolyte-Surfactant Complexes between Poly(vinylamine hydrochloride) and Oppositely Charged Sodium Alkyl Sulfate, *Macromolecules* 34 (2001) 1772-1778.
[28] S. Holappa, T. Andersson, L. Kantonen, P. Plattner, H. Tenhu, Soluble polyelectrolyte complexes composed of poly(ethylene oxide)-block-poly(sodium methacrylate) and poly(methacryloyloxyethyl trimethylammonium chloride), *Polymer* 44 (2003) 7907–7916.
[29] I. K. Voets, S. Burgh, B. Farago, R. Fokkink, D. Kovacevic, T. Hellweg, A. Keizer, M. A. C. Stuart, Electrostatically Driven Coassembly of a Diblock Copolymer and an Oppositely Charged Homopolymer in Aqueous Solutions, *Macromolecules* 40 (2007) 8476-8482.
[30] T. Matsuda, M. Annaka, Salt Effect on Complex Formation of Neutral/Polyelectrolyte Block Copolymers and Oppositely Charged Surfactants, *Langmuir* 24 (2008) 5707-5713.
[31] D. C. Gonzalez, E. N. Savariar, S. Thayumanavan, Fluorescence Patterns from Supramolecular Polymer Assembly and Disassembly for Sensing Metallo- and Nonmetalloproteins, *J. Am. Chem. Soc*. 131 (2009) 7708–7716.
[32] B. P. Bastakoti, S. Guragain, A. Yoneda, Y. Yokoyama, S. Yusa, K. Nakashima, Micelle

formation of poly(ethylene oxide-b-sodium 2-(acrylamido)-2-methyl-1-propane sulfonate-b-styrene) and its interaction with dodecyl trimethyl ammonium chloride and dibucaine, *Polym. Chem.* 1 (2010) 347–353.

[33] M. Monteserin, H. D. Burrows, R. Mallavia, R. E. Di Paolo, A. L. Mac-anita, M. J. Tapia, How to Change the Aggregation in the DNA/Surfactant/Cationic Conjugated Polyelectrolyte System through the Order of Component Addition: Anionic versus Neutral Surfactants, *Langmuir* 26 (2010) 11705–11714.

[34] P. Han, N. Ma, H. Ren, H. Xu, Z. Li, Z. Wang, X. Zhang, Oxidation-Responsive Micelles Based on a Selenium-Containing Polymeric Superamphiphile, *Langmuir* 26 (2010) 14414–14418.

[35] T. K. Bronich, A. Nehls, A. Eisenberg, V. A. Kabanov, A. V. Kabanov, Novel drug delivery systems based on the complexes of block ionomers and surfactants of opposite charge, *Colloids Surf. B: Biointerfaces* 16 (1999) 243-251.

[36] S. V. Solomatin, T. K. Bronich, T. W. Bargar, A. Eisenberg, V. A. Kabanov, A. V. Kabanov, Environmentally Responsive Nanoparticles from Block Ionomer Complexes: Effects of pH and Ionic Strength, *Langmuir* 19 (2003) 8069-8076.

[37] J. Wang, S. K. Varshney, R. Jerome, P. Teyssie, Synthesis of AB(BA), ABA and BAB block copolymers of *tert*-butyl methacrylate (A) and ethylene oxide (B), *J. Polym. Sci. Part A: Polym. Chem.* 30 (1992) 2251-2261.

[38] N. V. Nukolova, Z. Yang, J. O. Kim, A. V. Kabanov, T. K. Bornich, Polyelectrolyte nanogels decorated with monoclonal antibody for targeted drug delivery, *React. Funct. Polym*. 71 (2011) 315-323.

[39] M. Kamimura, N. Kanayama, K. Tokuzen, K. Soga, Y. Nagasaki, Near-infrared (1550nm) *in vivo* bioimaging based on rare-earth doped ceramic nanophosphors modified with PEG-*b*-poly(4-vinylbenzylphosphonate), *Nanoscale* 3 (2011) 3705-3713.

[40] K. P. Ananthapadmanabhan, E. D. Goddard, N. J. Turro, P. L. Kuo, Fluorescence Probes for Critical Micelle Concentration, *Langmuir* 1 (1985) 352-355.

[41] G. B.Ray, I. Chakraborty, S. P. Moulik, Pyrene absorption can be a convenient method for probing critical micellar concentration (cmc) and indexing micellar polarity, *J. Colloid Interface Sci.* 294 (2006) 248-254.

[42] T. K. Bronich, T. Cherry, S. V. Vinogradov, A. Eisenberg, V. A. Kabanov, A. V. Kabanov, Self-Assembly in Mixtures of Poly(ethylene oxide)-*graft*-Poly(ethyleneimine) and Alkyl Sulfates, *Langmuir* 14 (1998) 6101-6106.